Icarus 209 (2010) 535–541

Contents lists available at ScienceDirect

Icarus

journal homepage: www.elsevier.com/locate/icarus

Determining asteroid spin states using radar speckles

Michael W. Busch [a,*], Shrinivas R. Kulkarni [b], Walter Brisken [c], Steven J. Ostro [d,1], Lance A.M. Benner [d], Jon D. Giorgini [d], Michael C. Nolan [e]

[a] Division of Geological and Planetary Sciences, California Institute of Technology, Pasadena, CA 91125, United States
[b] Division of Physics, Mathematics, and Astronomy, California Institute of Technology, Pasadena, CA 91125, United States
[c] National Radio Astronomy Observatory, 1003 Lopezville Road, Socorro, NM 87801, United States
[d] Jet Propulsion Laboratory, California Institute of Technology, Pasadena, CA 91109-8099, United States
[e] Arecibo Observatory, HC3 Box 53995, Arecibo, PR 00612, United States

ARTICLE INFO

Article history:
Received 9 March 2010
Revised 5 May 2010
Accepted 12 May 2010
Available online 19 May 2010

Keywords:
Asteroids
Asteroids, Rotation
Asteroids, Dynamics
Radar observations

ABSTRACT

Knowing the shapes and spin states of near-Earth asteroids is essential to understanding their dynamical evolution because of the Yarkovsky and YORP effects. Delay-Doppler radar imaging is the most powerful ground-based technique for imaging near-Earth asteroids and can obtain spatial resolution of <10 m, but frequently produces ambiguous pole direction solutions. A radar echo from an asteroid consists of a pattern of speckles caused by the interference of reflections from different parts of the surface. It is possible to determine an asteroid's pole direction by tracking the motion of the radar speckle pattern. Speckle tracking can potentially measure the poles of at least several radar targets each year, rapidly increasing the available sample of NEA pole directions. We observed the near-Earth asteroid 2008 EV5 with the Arecibo planetary radar and the Very Long Baseline Array in December 2008. By tracking the speckles moving from the Pie Town to Los Alamos VLBA stations, we have shown that EV5 rotates retrograde. This is the first speckle detection of a near-Earth asteroid.

1. Introduction

Radar astronomy is a set of techniques for observing planets, comets, moons, and asteroids: transmitting from a ground station, receiving the echo, and resolving target objects in time delay (line-of-sight distance) and Doppler shift (line-of-sight velocity). Radar observations provide estimates of the near-surface bulk density and surface structure, precise trajectory predictions, and information on the target's shape, surface morphology, and rotation state comparable to that obtained by a close spacecraft flyby (Ostro et al., 2002).

The spin states of near-Earth asteroids (NEAs) are of particular interest. Asteroids' spin states are coupled to their orbits and shapes through the Yarkovsky and YORP effects. The Yarkovsky effect refers to the net effect of the radiation pressure produced by an object's thermal emission and is the largest single source of uncertainty in trajectory prediction of <2-km diameter asteroids that have been observed with radar (Ostro and Giorgini, 2004). The direction and magnitude of the Yarkovsky acceleration are determined by the object's surface temperature distribution, which is in turn determined by the orbit, pole direction, size, shape, albedo, and near-surface thermal inertia. Orbital integrations and direct measurements predict Yarkovsky-induced position offsets of millions of kilometers on timescales of decades to centuries when coupled with close planetary encounters (Giorgini et al., 2002, 2008; Chesley et al., 2003). Similarly, the YORP effect changes asteroid spin states on timescales of 10–100 kyr, with the radiation-pressure torque determined by the current orbit, shape, and spin state (Bottke et al., 2006). On timescales of >100 kyr, YORP can drive the fragmentation, orbital evolution, and coalescence of binary objects (Cuk and Burns, 2005; Scheeres, 2007; Walsh et al., 2008; Cuk and Nesvorny, 2010).

Shape reconstruction from delay-Doppler images has provided shape models and pole directions for about 30 asteroids (Benner, 2010). In many cases, the delay-Doppler data permit multiple shapes, often two solutions that are mirror images of each other but with opposite pole directions. This occurs because individual delay-Doppler images are ambiguous. For example, for a spherical object, each point in the northern hemisphere will have the same delay-Doppler position as one in the southern. Without extensive coverage in both sub-radar latitude and longitude (provided by significant sky motion and thorough rotation coverage), and high signal-to-noise ratio, ambiguous solutions result (e.g. Ostro et al., 2002; Busch et al., 2007; Brozovic et al., 2010). We have developed the technique of radar speckle tracking to overcome these ambiguities and provide another way to estimate pole directions.

* Corresponding author.
E-mail address: busch@caltech.edu (M.W. Busch).
[1] Deceased, 2008 December 15.

0019-1035/$ - see front matter © 2010 Elsevier Inc. All rights reserved.
doi:10.1016/j.icarus.2010.05.002

2. Radar speckles

On timescales of minutes, the radar echo flux received by an antenna is slowly varying and determined by the target object's size, shape, orientation, radar scattering properties, and distance from Earth. On short timescales (seconds or less), the echo oscillates randomly in brightness: a radar speckle pattern (Green, 1968; Kholin, 1988; Elachi and Van Zyl, 2006; Margot et al., 2007). Each point on the surface of the asteroid reflects the incident radar wave differently and acts as a radiator with random phase. Viewed from the Earth, the radiation from each pair of points will interfere to produce a sinusoidal pattern of bright and dark speckles, as seen in Young's classic double-slit experiment. The points with the largest projected separation will produce the smallest speckles, with angular scale λ/d, where d is the diameter of the target and λ is the radar wavelength. The speckles from all possible pairs of points add together randomly to produce the speckle pattern received at the Earth, where the smallest speckles have length:

$$L_{Speckle} = r\lambda/d \tag{1}$$

for a target a distance r away (Fig. 1).

The speckle pattern is determined by the object's radar scattering properties and shape on all spatial scales larger than a fraction of a wavelength. In principle, sampling the entire pattern would permit a full reconstruction of the shape (Kholin, 1988). That would require an implausibly large number of independent receiving stations (see Supplementary Material 2). In practice, we are limited to measuring the speckles received at a small number of locations, insufficient to do more than measure $L_{Speckle}$. However, there is information in how the speckles change with time. As the asteroid rotates, the distance from the radar to each point on the surface changes, changing their relative phases and rotating the speckles in the same direction as the surface. On longer timescales (typically minutes), the speckles change in pattern as the incidence angle, and hence the radar scattering, at each point on the asteroid's surface changes.

Stations with a separation projected normal to the line of sight (a baseline, Fig. 1) larger than $L_{Speckle}$ will receive series of speckles that are not, in general, correlated with each other (Kholin, 1988). This means that multiple receive stations for plane-of-sky interferometric imaging of radar targets, which several authors have proposed (Supplementary Material 2, Black et al., 2005; Busch et al., 2008), is not possible. However, if two stations are fortuitously aligned in the direction of speckle motion *or* spaced much closer together than the speckle scale, we can still determine the target's sense of rotation. Speckles from prograde-rotating asteroids will move from east to west, and those from retrograde rotators from west to east. Thus the motion of the speckle pattern indicates the sense of rotation.

We determine the direction of speckle motion by cross-correlating the echo power (*not* the complex-valued voltage functions used in interferometry) received at two stations, separated by a baseline of length B, to determine the relative time lag t_{lag} – the difference in arrival time of a speckle between the stations. The sign of t_{lag} indicates the asteroid's sense of rotation. The projected speckle speed $|B/t_{lag}|$ is determined by the asteroid's rotation period P, the latitude θ of the sub-Earth point on the asteroid, and the angle α between the asteroid's spin vector projected on the sky and the baseline (Green, 1968; Kholin, 1992; Margot et al., 2007). Typical speckle velocities for near-Earth asteroids with rotation periods shorter than tens of hours are >1000 km/s during radar tracks (Eq. (2)), so we may ignore the contributions from the Earth's rotation (<0.5 km/s) and the relative motion of the Earth and the target (always <90 km/s, usually <10 km/s):

$$|B/t_{lag}| \approx \frac{2\pi r\cos(\theta)}{P\sin(\alpha)} \tag{2}$$

For very close-approaching (low r) or slowly-rotating (high P) radar targets, Eq. (2) ceases to be a good approximation, and Earth's rotation and the relative motion must be subtracted from the observed velocity to obtain the true speckle speed. For example, 4179 Toutatis has $P > 100$ h (Hudson and Ostro, 1995), and will have speckle velocity ~130 km/s at $r = 0.046$ AU during its Earth approach in 2012, as compared to a contribution of 12 km/s from the asteroid–Earth velocity. Given optical lightcurves and/or a detailed series of delay-Doppler radar images and the asteroid's known orbit, P and r are known. The magnitude of t_{lag} therefore corresponds to one dimension of the asteroid's pole direction (the angle α).

Multiple baselines at appropriate separations, different angles, and different times give the asteroid's complete spin vector (Green, 1968), limited by the uncertainties in measuring the different t_{lag} values. The direction of the spin vector (the pole direction) is the direction that gives the appropriate values of α for all the baselines. Similarly, with multiple baselines, P can be estimated in the absence of lightcurve data (although when available, lightcurves can provide much more precise period measurements). At least three baselines are required for a unique measurement of the spin vector by speckle tracking alone. These baselines can be between either the same or different pairs of stations, but must be at different times so that the target has moved and the sub-Earth latitude and projected spin axis have changed.

The maximum cross-correlation amplitude between two stations is determined by the radar echo's strength and the collecting areas and system temperatures of the two receiving antennas, but most importantly by the baseline length projected along the direction of speckle motion. For $B\cos(\alpha) < L_{Speckle}$, where cross-correlation is possible, the relationship between the correlation amplitude and the projected baseline length is very roughly (Kholin, 1992):

$$C = e^{-2(B\cos(\alpha)/L_{Speckle})^2} \tag{3}$$

This very strong dependence on baseline length means that baselines much shorter than the speckle scale are required, unless α happens to be close to 90°.

The cross-correlation as a function of time lag is a continuously varying function, with peaks with width in time approximately equal to the speckle duration $(L_{Speckle})/|B/t_{lag}| = \lambda P/(2\pi d)$. Smaller changes in time lag only partially shift speckles into or out of correlation with each other. Fortunately, if the correlation amplitude is much larger than the noise on it, t_{lag} can be determined to much less than the peak width.The 1-σ uncertainty in t_{lag} is

$$\Delta t_{lag} = \frac{1}{\sqrt{cor\mathrm{SNR}}}\frac{\lambda P}{2\pi d} \tag{4}$$

$$\text{where} \quad cor\mathrm{SNR} = C\frac{P_{Eff}}{kT_{Eff}}b^{1/2}t_{Int}^{1/2}$$

$$\text{and} \quad P_{Eff} = \frac{P_T G_T \sigma}{(4\pi)^2 r^4}\left(\frac{A_1 A_2}{A_1 + A_2}\right)$$

The correlation signal-to-noise ratio (*cor*SNR) is determined by the overall correlation amplitude, the effective echo power (P_{Eff}), the echo bandwidth (b), the integration time (t_{Int}), and the effective temperature of the receivers (here assumed to be the same for both stations). The effective echo power is the product-over-sum of the echo power received at the two stations, and is determined by the transmitter power (P_T) and gain (G_T), the distance to the target and its radar cross-section (σ), and the effective areas of the antennas (A_1 and A_2). The expression for P_{Eff} is the interferometric version of the well-known radar equation (e.g. Ostro et al., 2002).

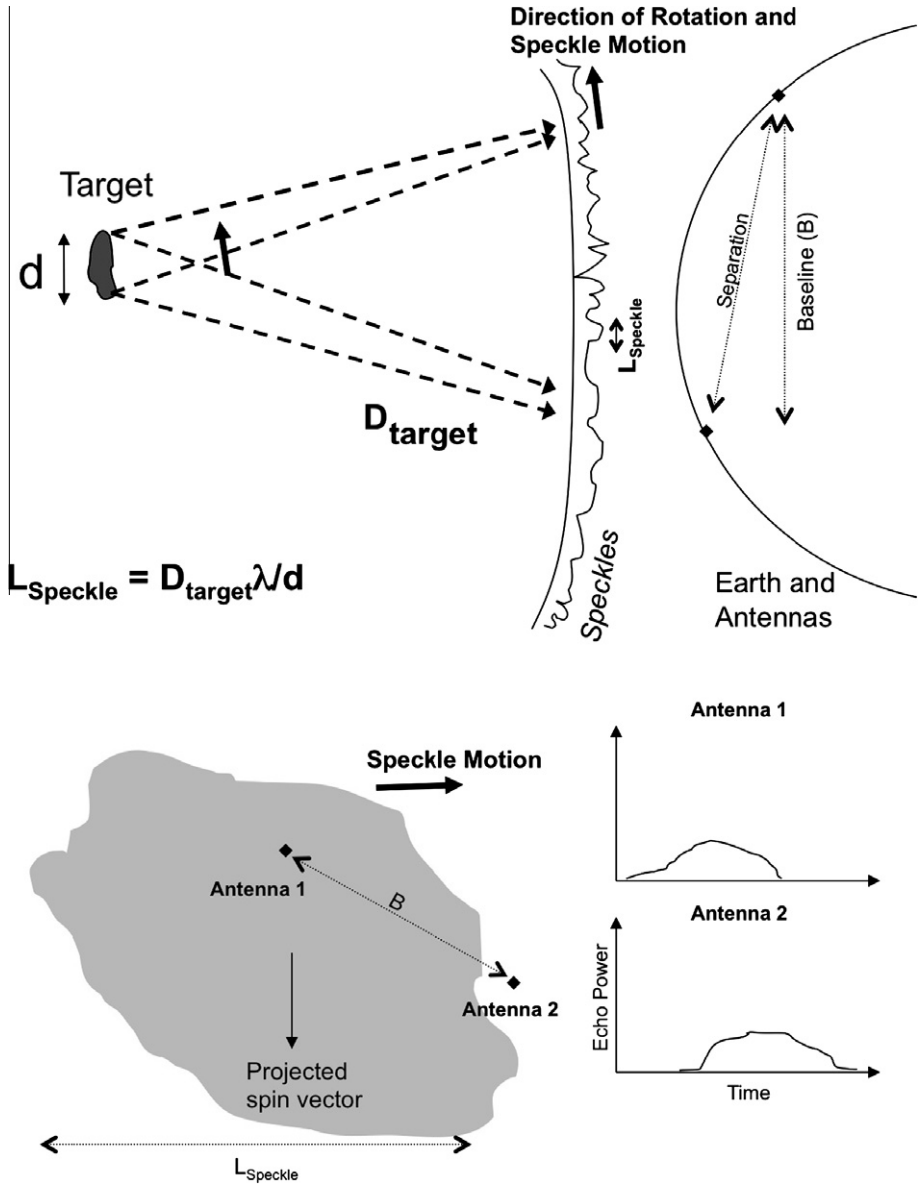

Fig. 1. Schematic of a radar speckle pattern (not to scale). *Top.* The reflected light from each point on the target's surface forms a wavefront and these interfere constructively or destructively, producing the random pattern of bright and dark speckles at the Earth, intercepted by a pair of antennas with some baseline. As the asteroid rotates, the phase at each point on the surface changes, moving the speckles in the same direction as the surface. *Bottom.* A single bright speckle passing over two antennas with baseline $B < L_{Speckle}$ and the echo power at each as a function of time. The average difference in arrival time over many speckles is equal to t_{lag}. Figure based on that in Green (1968).

The uncertainty in a time lag measurement cannot be converted blindly into the uncertainty in a measurement of α. Two nearby stations will see a series of speckles that are correlated with each other, but are not identical. For example, an elliptical speckle would both last longer and peak at a different time as viewed by a station that sees its center as compared to one offset to the side (Fig. 1). This introduces systematic errors into t_{lag}, which can be decreased by averaging and by using shorter baselines where the speckles are more similar to each other. In the limit of zero systematics, the uncertainty in α will be $\approx \Delta t_{lag}/t_{lag}$.

3. Test case: 2008 EV5

2008 EV5 (hereafter EV5) was discovered on 2008 March 4 by the Mount Lemmon Survey (Larson et al., 2006). It passed within 8.4 lunar distances (0.023 AU, 1.3×10^6 km) of Earth on 2008 December 23, and was therefore a very strong target for radar observations. We observed EV5 using the Goldstone 8560 MHz (3.5-cm) radar over 2008 December 16–23 and the Arecibo 2380 MHz (12.6-cm radar) over 2008 December 23–27. The data consist primarily of delay-Doppler images, which show that EV5 is a 450 ± 40 m oblate spheroid (Fig. 2). The radar observations and shape modeling will be described in more detail in a separate paper by Busch et al. (in prep.). The delay-Doppler data permit two possible pole directions – prograde and retrograde mirror images – making EV5 an ideal test case for speckle tracking.

During the December 23 Arecibo observations, we transmitted a pure tone from Arecibo and received echoes with 9 of the 10 stations of the Very Long Baseline Array (VLBA) and the Green Bank telescope (GBT). These data were transferred to the NRAO Array Operations Center in Socorro, New Mexico, and processed using a special-purpose correlator program written by one of the authors (M.W. Busch). As a check, we also processed the EV5 data using

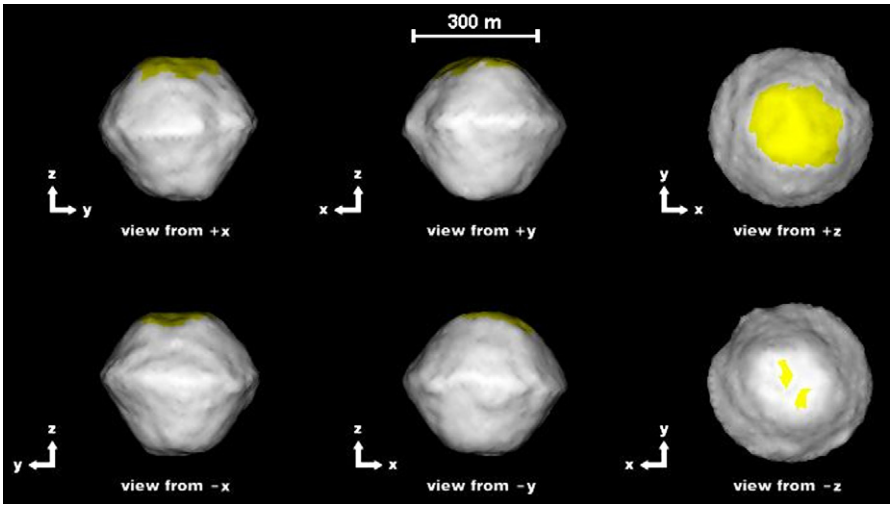

Fig. 2. Principal axis views of our shape model of 2008 EV5 (for the delay-Doppler-derived retrograde pole direction). The yellow shading denotes areas that were not visible at incidence angles less than 60°. This shape may not reflect EV5's true topography, but the equatorial ridge and the accompanying concavity are obvious in the delay-Doppler images. The exact latitude of the ridge and the position of the depression are uncertain; the ridge may lie at any latitude between 30°N (+z) and 30°S (−z). Figure adapted from a companion paper by Busch et al. (in preparation).

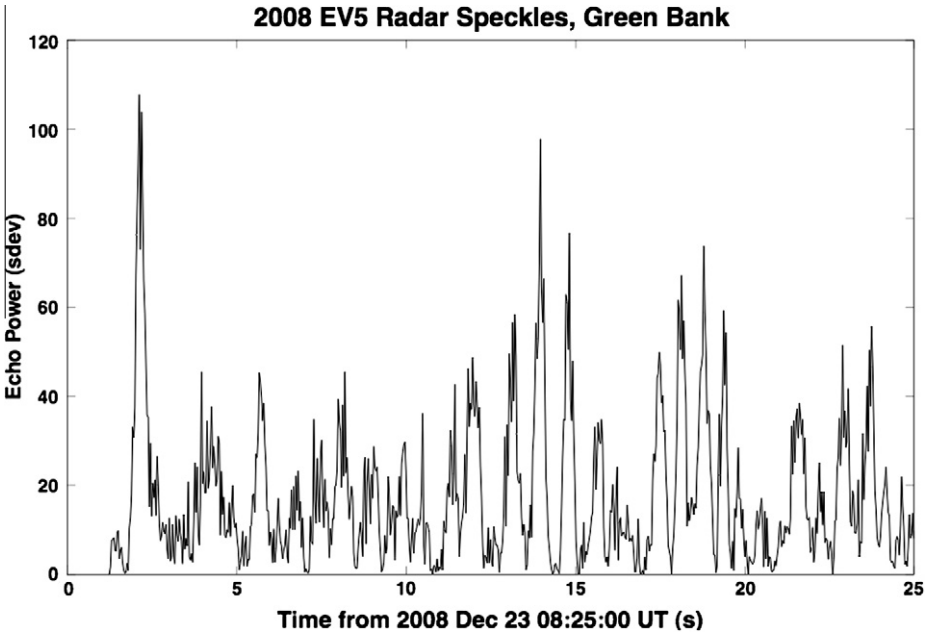

Fig. 3. 2008 EV5 radar echo power received by Green Bank as a function of time on 2008 December 23, with 0.025 s resolution, showing speckles moving over the station. Given a speckle scale of 900 km, the average speckle duration of 0.65 ± 0.05 s gives a speckle velocity of 1350 ± 150 km/s, as expected from EV5's distance and rotation rate. The point-to-point variations in echo power are self-noise due to the small number of Fast Fourier Transforms in each measurement. The data were processed using the special purpose software correlator written for this work. Time resolution is 0.025 s; the echo arrived at the telescope starting at 08:25:01.30 UT.

the NRAO's version of the DiFX software correlator (Deller et al., 2007). The two programs produce nearly identical results (Supplementary Fig. 1).

The correlator obtains the echo power received by each station as a function of time, clearly showing individual speckles (Fig. 3). As described in Section 2, we cannot use the speckle pattern to obtain EV5's detailed shape, but it is consistent with a surface that is rough on the scale of the radar wavelength (Supplementary Fig. 2). The speckle timescale is 0.65 ± 0.05 s, consistent with EV5's diameter of 450 ± 40 m and rotation period of 3.725 ± 0.001 h (Galad et al., 2009). By cross-correlating the echo power received at two different stations with the signals shifted by all possible values of t_{lag}, we determine the direction and velocity of speckle motion.

For speckle cross-correlation, we considered the closest VLBA antenna pairs: Pie Town (PT) and Los Alamos (LA), New Mexico; Kitt Peak (KP), Arizona; and Fort Davis (FD), Texas. The shortest baseline during our EV5 observations was Pie Town to Los Alamos (PT–LA): 235 km. The highest cross-correlation was obtained at PT–LA $t_{lag} = -0.17 \pm 0.05$ s. The speckles moved from west to east, arriving at Pie Town first (Fig. 4). Therefore, EV5 has a *retrograde* pole direction.

The projected speckle velocity along PT–LA was $|B/t_{lag}| = 1380(+700\ -500)$ km/s, implying that the baseline was angled at

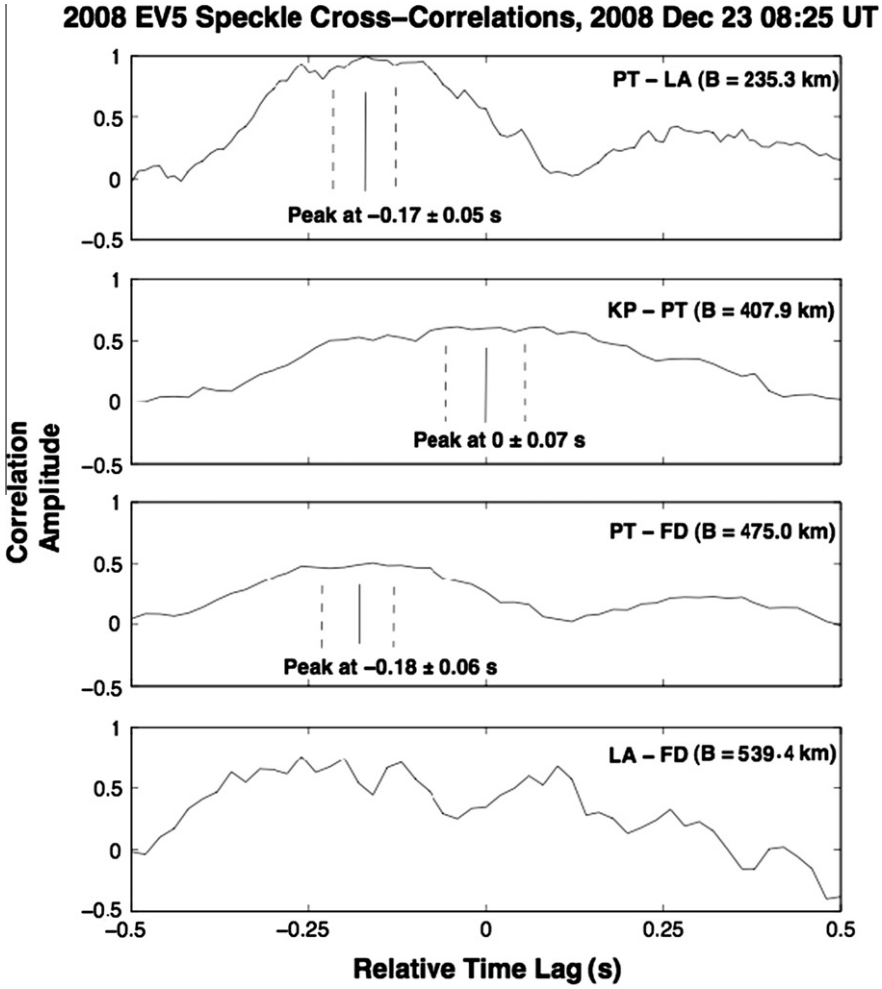

Fig. 4. Cross-correlation of the echo power received at four closest pairs of VLBA stations as a function of relative time lag. Labels give stations and baseline lengths (PT = Pie Town, LA = Los Alamos, FD = Fort Davis, KP = Kitt Peak). t_{lag} was sampled at 0.01 s intervals. The peaks in correlation amplitude at negative t_{lag} indicate retrograde rotation, and are consistent with EV5's rotation period and the angles between the spin axis and the baselines. The KP-PT baseline was aligned almost at right angles to the speckle motion, so that t_{lag} is indistinguishable from zero (see text). The secondary peaks are due to speckles moving into and out of correlation with each other, and have width approximately equal to the speckle duration (0.65 s). The uncertainties in our estimates of the position of the peaks include upper limits on systematic errors. For LA-FD the correlation peak is too weak for a fit to be meaningful.

$\alpha = 90^\circ$ ($+0\ -40^\circ$) relative to EV5's rotation axis (90° corresponds to 1350 km/s). This is consistent with the retrograde pole direction estimated by inverting the delay-Doppler data (Busch et al., in preparation), which predicts $\alpha = 62 \pm 5^\circ$.

The second- and third-shortest VLBA baselines (KP–PT and PT–FD) also show peaks in cross-correlation, but they are weaker and have correspondingly larger uncertainties (Fig. 4). This is expected from Eq. (3). For $B\cos(\alpha) = 450$ km $= (L_{Speckle}/2)$, the cross-correlation amplitude between stations should drop by ~40% as compared to a baseline of nearly zero length. The KP-PT and PT–FD baselines were between 400 and 500 km, so they had weaker cross-correlations than PT–LA. All the other baselines in the array (LA–FD and longer) do not have strong cross-correlations.

The PT–FD cross-correlation has significantly higher signal-to-noise-ratio than that for KP–PT, despite the somewhat larger B and lower correlation amplitude. This reflects lower system temperature at Fort Davis. The time lags along the KP–PT and PT–FD baselines are consistent with the retrograde pole direction estimated from the delay-Doppler data. Given that pole direction, PT–FD had $\alpha \approx 38 \pm 5^\circ$, while KP–PT had $\alpha \approx 13 \pm 5^\circ$, producing a t_{lag} indistinguishable from zero. This demonstrates the need for multiple baselines: if the pole direction is unknown, α on any given baseline may be small.

The uncertainties in our measurements of t_{lag} are conservative and include an upper limit of the systematic error from the differences between the speckles as seen by the two stations. The systematic uncertainty in t_{lag} as measured by a single speckle is comparable to or less than the speckle duration, and will average down as square root of the number of speckles. The cross-correlations each included ~250 speckles with duration ~0.65 s, so the systematic error will be $<\sim 0.042$ s. Adding the systematic error in quadrature with the formal $\Delta t_{lag} = 0.018$ s gives an overall uncertainty of $\leqslant 0.05$ s.

4. Implications

As described above, inversion of delay-Doppler images can, in some instances, yield unambiguous pole directions, but for many NEAs this is not possible due to insufficient sky motion of the target and inadequate rotation coverage. Spin state ambiguities limit what we can say about an object. The most dramatic example of a spin state ambiguity is the NEA (29075) 1950 DA: delay-Doppler images obtained in 2001 allow two pole solutions; if the prograde solution is correct, then 1950 DA could impact Earth in 2880 due to the Yarkovsky effect (Giorgini et al., 2002; Busch et al., 2007). If

Table 1
Preferred antenna pairs for speckle tracking.

Antennas						Separation (km)	Sensitivity/VLBA
Goldstone	70-m	USA	DSS	24, 25, 26, 34-m	USA	10	2.8
Goldstone	70-m	USA	DSS	13, 34-m	USA	22	2.8
Usuda	64-m	Japan	Nobeyama	45-m	Japan	28	3.3
Jodrell Bank	76-m	UK	Cambridge	32-m	UK	198	2.6
Goldstone	70-m	USA	Owens	40-m	USA	233	3.1
Canberra	70-m	Australia	Parkes	64-m	Australia	274	6.3
Effelsberg	100-m	Germany	Cambridge	32-m	UK	510	2.6
Effelsberg	100-m	Germany	Jodrell Bank	76-m	UK	700	11.7

Combinations of antennas for radar speckle tracking sorted by separation (maximum baseline length). The separations given here have been rounded to the nearest 1 km and are the straight-line distances between the antennas. During an observation, the baseline length decreases depending on the direction to the target, due to foreshortening. Only separations less than 1000 km are listed here. The preferred baseline length depends on the target object (see text). The choice of antennas is also constrained by the location of the transmitter; e.g. sites in Australia can only view Goldstone radar targets.
Sensitivities are given as ratios of (speckle correlation SNR for antenna pair)/(speckle correlation SNR for two VLBA stations) for the same target and are approximate. The table lists the most sensitive baseline pairs. A more extensive version is provided as Supplementary Table 1.
This list contains antennas that could potentially be used for speckle tracking. Effelsberg in particular would require significant preparation before any speckle observations. DSS refers to antennas at Deep Space Network Sites, located at the Goldstone Deep Space Communications Complex. See Supplementary Table 1 for references and antenna properties.

speckle tracking had been available at the time of the 2001 observations, we would not have to wait for Lightcurve observations (in 2012 and 2023) or the next opportunity for radar observations (in 2032) to resolve the ambiguity.

The success of the EV5 speckle observations and the example of 1950 DA motivate observing the speckle patterns of as many strong radar targets as possible.

4.1. Observing requirements

As described above, the baseline length must be much less than the speckle scale for reliable speckle tracking. In addition, there is a minimum useful baseline length: the distance for which t_{lag} becomes comparable to its uncertainty. For very short baselines, the systematic errors in t_{lag} will be small compared to Δt_{lag}:

$$\begin{aligned} B &\ll L_{Speckle} \\ B &\gg (2\pi r/P)\Delta t_{lag} \end{aligned} \tag{5}$$

For shorter baselines, t_{lag} is indistinguishable from zero and there is no information on the pole direction. For longer baselines, speckle tracking is only possible if the baseline is aligned along the direction of speckle motion ($\alpha \approx 90°$). This can be planned for objects with a known pole direction; as used by Margot et al. (2007) to measure Mercury's spin state. However, for new asteroid radar targets the use of baselines with $B > L_{Speckle}$ is strictly a matter of luck, with the probability of a strong cross-correlation being $\ll r\lambda/dB$ for a random pole direction. Reliable speckle tracking requires baselines in the range given by Eq. (5).

In addition to speckle tracking being more useful for shorter baselines, stronger echoes provide better measurements of t_{lag}, so the utility of speckle measurements is proportional to the sensitivity of the receiving antennas. In both respects, the 25-m VLBA stations are not ideal. EV5 was one of the strongest radar targets at Arecibo in 2008, but the SNR of the PT–LA cross-correlation is only ≈ 10. There are several larger antennas that provide both higher sensitivity and appropriate baselines (Table 1, Supplementary Table 1, Grueff et al., 2004). With high sensitivity, speckle measurements of the spin state can be an order of magnitude more accurate than measurements from delay-Doppler imaging, as previously demonstrated for Mercury (Margot et al., 2007).

While planning observations of new radar targets, appropriate baselines must be identified. However, diameter estimates from optical photometry have uncertainties of roughly a factor of two and the maximum and minimum useful baseline length will be uncertain by that factor as well. For most strong radar targets, this leaves a range of useful baselines between tens and hundreds of kilometers. For the smallest objects ($d \ll 100$ m at $r < 0.01$ AU), baselines around 1000 km are useful: the speckle scales are larger, and rapid rotation (low P) frequently excludes short baselines.

4.2. Measuring asteroid pole directions

Knowing asteroid spin states is essential for long-term trajectory prediction of small (diameter $< \sim 2$ km) NEAs. The Yarkovsky and YORP effects influence the orbits, rotation periods, pole directions, and shapes of individual NEAs. Improved pole direction estimates will provide more accurate Yarkovsky predictions, and successful Yarkovsky acceleration detections yield estimates of the target's mass, bulk density, and near-surface thermal inertia. Improved YORP predictions will illuminate the spin state histories of the NEAs.

The Yarkovsky effect may also influence the overall properties of the NEA population. Based on a sample size of only 20 objects, La Spina et al., 2004 found a non-uniform distribution of NEA pole directions, with an excess of retrograde rotators. Retrograde spins may preferentially drive Yarkovsky migration from the main-belt into resonances with Jupiter and Saturn that inject these objects into Earth-crossing orbits (Kryszczynska et al., 2007). To test this hypothesis, we must estimate pole directions for many more objects. Speckle tracking can provide that information, potentially measuring the poles of ten or more radar targets each year, significantly more than are estimated from inversion of delay-Doppler images, so that within a few years the sample of NEA pole directions could be more than doubled.

For the strongest radar targets ($\sim$2/year), speckle tracking can measure pole directions to $<1°$ (e.g. a 150-m object at 0.01 AU observed with transmission from Arecibo and receiving at Jodrell Bank and Effelsberg). With sub-degree measurements at multiple epochs in combination with lightcurve and delay-Doppler data, it may be possible to directly track small changes in asteroid pole directions; produced by YORP, collisions, shape changes due to tidal forces during planetary encounters (such as 99942 Apophis' 5.6 Earth-radii flyby in 2029, Scheeres et al., 2005), or tidal interactions in binary systems – such as the precession of the spin axis of 1999 KW4 Alpha (Ostro et al., 2006; Scheeres et al., 2006). For objects in non-principal axis rotation states (wobbling or tumbling), such as Toutatis, speckle tracking can provide accurate measurements of the instantaneous spin vectors on several days. In combination with lightcurves to estimate the rotation and precession periods and delay-Doppler imaging to estimate the shape, these would provide the moments of inertia and information about the internal

mass distribution (Hudson and Ostro, 1995), testing our understanding of NEA formation.

These applications demonstrate the utility of speckle tracking. We plan for it to become a routine part of future asteroid radar observations.

Acknowledgments

The NRAO Socorro & Green Bank, Goldstone Solar System Radar, and NAIC Arecibo staff helped to obtain the data presented here. A. Galad, B.W. Koehn, and M.D. Hicks observed EV5 optically and determined its rotation rate. J.-L. Margot and C. Magri provided very helpful reviews. A.T. Deller and R.C. Walker provided helpful technical comments. The National Radio Astronomy Observatory is a facility of the National Science Foundation operated under cooperative agreement by Associated Universities, Inc. The Arecibo Observatory is part of the National Astronomy and Ionosphere Center, which is operated by Cornell University under a cooperative agreement with the National Science Foundation. Some of this work was performed at the Jet Propulsion Laboratory, California Institute of Technology, under contract with the National Aeronautics and Space Administration (NASA). This paper is based in part on work funded by NASA under the Science Mission Directorate Research and Analysis Programs. M.W. Busch was supported by the Hertz Foundation.

Appendix A. Supplementary material

Supplementary data associated with this article can be found, in the online version, at doi:10.1016/j.icarus.2010.05.002.

References

Benner, L.A.M., 2010. Asteroid 3-D Shape Models Estimated from Delay-Doppler Radar Data. <http://echo.jpl.nasa.gov/~lance/shapes/asteroid_shapes.html>.

Black, G., Campbell, D.B., Treacy, R., Nolan, M.C., 2005. Radar-interferometric asteroid imaging using a flexible software correlator. Bull. Am. Astron. Soc. 37, 1155.

Bottke, W.F., Vokrouhlicky, D., Rubincam, D.P., Nesvorny, D., 2006. The Yarkovsky and YORP effects: Implications for asteroid dynamics. Annu. Rev. Earth Planet. Sci. 34, 157–191.

Brozovic, M., Benner, L.A.M., Magri, C., Ostro, S.J., Scheeres, D.J., Giorgini, J.D., Nolan, M.C., Margot, J.-L., Jurgens, R.F., Rose, R., 2010. Radar observations and a physical model of contact binary Asteroid 4486 Mithra. Icarus 208, 207–220.

Busch, M.W., and 15 colleagues, 2007. Physical modeling of near-Earth Asteroid (29075) 1950 DA. Icarus 190, 608–621.

Busch, M.W., Ostro, S.J., Kulkarni, S.R., Brisken, W.F., Nolan, M.C., 2008. Radar interferometric imaging of near-Earth objects. Bull. Am. Astron. Soc. 40, 437.

Busch, M.W., and 14 colleagues, 2010. The shape of 2008 EV5: Craters and ridges on near-Earth asteroids, in preparation.

Chesley, S.R., Ostro, S.J., Vokrouhlicky, D., Capek, D., Giorgini, J.D., Nolan, M.C., Margot, J.-L., Hine, A.A., Benner, L.A.M., Chamberlin, A.B., 2003. Direct detection of the Yarkovsky effect by radar ranging to Asteroid 6489 Golevka. Science 302, 1739–1742.

Cuk, M., Burns, J.A., 2005. Effects of thermal radiation on the dynamics of binary NEAs. Icarus 176, 418–431.

Cuk, M., Nesvorny, D., 2010. Orbital evolution of small binary asteroids. Icarus 207, 732–743.

Deller, A.T., Tingay, S.J., Bailes, M., West, C., 2007. DiFX: A software correlator for very long baseline interferometry using multiprocessor computing environments. Proc. Astron. Soc. Pac. 119, 318–336.

Elachi, C., Van Zyl, J., 2006. Introduction to the Physics and Techniques of Remote Sensing, second ed. John Wiley & Sons, Hoboken. pp. 242.

Galad, A., Vilagi, J., Kornos, L., Gajdos, S., 2009. Relative photometry of nine asteroids from Modra. Minor Planet Bull. 36, 116–118.

Giorgini, J.D., and 13 colleagues, 2002. Asteroid 1950 DA's encounter with Earth in 2880: Physical limits of collision probability prediction. Science 296, 132–136.

Giorgini, J.D., Benner, L.A.M., Ostro, S.J., Nolan, M.C., Busch, M.W., 2008. Predicting the Earth encounters of (99942) Apophis. Icarus 193, 1–19.

Green, P.E., 1968. Radar measurements of target scattering properties. In: Evans, J.V., Hagfors, T. (Eds.), Radar Astronomy. McGraw-Hill, New York, pp. 1–19.

Grueff, G., Alvito, G., Ambrosini, R., Bolli, P., Maccaferri, A., Maccaferri, G., Morsiani, M., 2004. Sardinia radio telescope: The new Italian project. Proc. SPIE 5489, 773.

Hudson, R.S., Ostro, S.J., 1995. Shape and non-principal axis spin state of Asteroid 4179 Toutatis. Science 270, 84–86.

Kholin, I.V., 1988. Spatial–temporal coherence of a signal diffusely scattered by an arbitrarily moving surface for the case of monochromatic illumination. Radiophys. Quant. Electron. 31, 371–374 (translation from Russian original).

Kholin, I.V., 1992. Accuracy of body-rotation-parameter measurement with monochromatic illumination and two-element reception. Radiophys. Quant. Electron. 35, 284–287 (translation from Russian original).

Kryszczynska, A., La Spina, A., Paolicchi, P., Harris, A.W., Breiter, S., Pravec, P., 2007. New findings on asteroid spin-vector distributions. Icarus 192, 223–237.

La Spina, A., Paolicchi, P., Kryszczynska, A., Pravec, P., 2004. Retrograde spins of near-Earth asteroids from the Yarkovsky effect. Nature 428, 400–401.

Larson, S.M., Beshore, E.C., Christensen, E.J., Hill, R.E., Kowalski, R.A., Gibbs, A.R., Odell, A.P., McNaught, R.H., Garradd, G.J., Grauer, A.D., 2006. The status of the Catalina Sky Survey for NEOs. Bull. Am. Astron. Soc. 38, 592.

Margot, J.-L., Peale, S.J., Jurgens, R.F., Slade, M.A., Holin, I.V., 2007. Large longitude libration of Mercury reveals a molten core. Science 316, 710–714.

Ostro, S.J., Hudson, R.S., Benner, L.A.M., Giorgini, J.D., Magri, C., Margot, J.-L., Nolan, M.C., 2002. Asteroid radar astronomy. In: Bottke, W.F., Cellino, A., Paolicchi, P., Binzel, R.P. (Eds.), Asteroids III. University of Arizona Press, Tucson, pp. 151–168.

Ostro, S.J., Giorgini, J.D., 2004. The role of radar in predicting and preventing asteroid and comet collisions with Earth. In: Belton, M.J.S., Morgan, T.H., Samarasinha, S.H., Yeomans, D.K. (Eds.), Mitigation of Hazardous Comets and Asteroids. Cambridge University Press, Cambridge, pp. 38–65.

Ostro, S.J., and 15 colleagues, 2006. Radar imaging of binary near-Earth Asteroid (66391) 1999 KW4. Science 314, 1276–1280.

Scheeres, D.J., Benner, L.A.M., Ostro, S.J., Rossi, A., Marzari, F., Washabaugh, P., 2005. Abrupt alteration of Asteroid 2004 MN4's spin state during its 2029 Earth flyby. Icarus 178, 281–283.

Scheeres, D.J., and 15 colleagues, 2006. Dynamical configuration of binary near-Earth Asteroid (66391) 1999 KW4. Science 314, 1280–1283.

Scheeres, D.J., 2007. Rotational fission of contact binary asteroids. Icarus 189, 370–385.

Walsh, K.J., Richardson, D.C., Michel, P., 2008. Rotational breakup as the origin of small binary asteroids. Nature 454, 188–191.